Desalination and Water Treatment
www.deswater.com

doi: 10.1080/19443994.2016.1150208

57 (2016) 25800–25811
November

Taylor & Francis
Taylor & Francis Group

Methylene blue dye degradation using C-100 polymeric material modified with ZnO nanoparticles

Medhat Mohamed El-Moselhy

Faculty of Science, Chemistry Department, Al-Azhar University, Nasr city, Cairo 11884, Egypt, Tel. +20 1006292802; email: medhatmohamed@yahoo.com

Received 11 October 2015; Accepted 31 January 2016

ABSTRACT

In this work, ZnO nanoparticles were incorporated inside C-100 as a kind of ion exchange material by impregnation with 8% $Zn(CH_3COO)_2$ solution. The modified material after Zn^{2+} loading was then treated with a solution of 5% sodium hydroxide to precipitate zinc hydroxide species on the surface of the C-100 exchanger as well as inside the internal pores of the polymeric matrix. After precipitation of zinc hydroxide, the materials were exposed to roasted vapor for an hour on the intermittent periods of time to form a zinc oxide. The synthesized samples with different ZnO loadings were denoted as Zn-HCIX and characterized using X-ray diffraction, energy-dispersive X-ray spectroscopy, scanning electron microscope, and the tunneling electron microscope. The synthesized materials were applied in the photocatalytic degradation of methylene blue dye in aqueous medium using UV irradiation (λ = 254 nm) under different experimental conditions. The data obtained indicate that the synthesized materials possess a very good adsorption capacity as well as excellent catalytic activity toward the removal of methylene blue.

Keywords: ZnO nanoparticles; Ion exchange; Methylene blue; Adsorption and photodegradation

1. Introduction

In recent years, due to human activities, the presence of dyes is common in wastewater coming out from industrial effluent of different industries such as textile, leather, foodstuff, and cosmetics [1–11]. The presence of organic pollutants in wastewater can cause a serious health problem. Due to the lack of water resources, the process of wastewater treatment has attracted the attention of researchers to find out a suitable way for the complete mineralization of such kind of wastes. Different techniques have been used to examine the removal process depending on the nature and stability of the dyes. Adsorption processes play an important role in the removal process, but with the lower concentration range due to the fast surface coverage in case of high dye concentration in the effluent [12–16]. Furthermore, the regeneration of the adsorbent represents another issue and required excessive work. The photocatalytic degradation techniques have been extensively used as an example for the advanced oxidation processes, in which a catalyst is used for the mineralization of the organic pollutants. The efficiency of the degradation process depends mainly on the choice of catalyst as well as the working experimental conditions. There are a big number of photocatalysts that could be used for the degradation of organic wastes. Several kinds of

metal oxides are known in the field of water treatment using advanced oxidation techniques such as TiO_2, ZnO, and ZnS exhibiting excellent photocatalytic activity. Several works indicate the complete mineralization of organic dyes in a very short time and normal experimental conditions. The use of zinc oxide as one of the photocatalysts for the photodegradation of organic compounds is of great importance to many researchers [16–19]. The preparation of zinc in the form of nanostructure is very simple, inexpensive and does not require high calcination temperatures. Moreover, the results given by the zinc oxide showed high efficiency cracking which could match or exceed the efficiency of titanium dioxide.

The process of catalyst recycling is not easy especially when the photocatalyst is powder. The presence of photocatalyst in the treated stream might cause another issue since it requires further treatment process depending on the amount and size of the photocatalyst used. Furthermore, the process of regeneration and reuse of the photocatalyst is very difficult. To avoid catalyst filtration problems, the development of new techniques has arisen, including the support of photocatalyst on a solid surface to save a great surface area and high dose of catalyst with no catalyst dissolution in the treated stream [20,21]. In our laboratory, we developed a new technique based on the supporting of the photocatalyst on a particular kind of commercial polymeric materials to facilitate the recycling and reuse of the catalyst.

In this work, the incorporation of Zn ions was carried out on macroporous cation exchanger (C-100) via ion exchange processes followed by precipitation of loaded Zn ions as $Zn(OH)_2$ which then followed by hydrothermal treatment using roasted air to form ZnO species. The catalytic activity of the synthesized materials will examine the photodegradation of methylene blue dye (MB). The modified polymeric material possesses high surface area that accesses a high Zn content reaching ≈400 mg Zn/g C-100, resistant to attrition and easier recycling and reuse for unlimited number of cycles. Furthermore, the loaded Zn is strongly attached to the polymeric matrix which prevents the easier dissolution of zinc during the degradation reaction.

2. Materials and methods

2.1. Materials

MB with the molecular formula ($C_{16}H_{18}N_3SCl$) and 98% purity, sodium hydroxide, zinc acetate and hydrochloric acid were purchased from Merck. AR grade was used as received without further purification.

The used cation exchanger (Purolite C-100) are of industrial grade, premium gel, polystyrenic, strong acid cation exchange resins supplied in sodium and hydrogen form, respectively.

2.2. Synthesis of catalyst

20 g of C-100 was treated with 8% $ZnCl_2$ at pH 6 and agitated for 20 h at room temperature using a handmade mechanical shaker. The modified resin was washed and treated with 5% NaOH solution to form $Zn(OH)_2$ followed by washing with distilled water several times to remove the excess of NaOH. The previous processes were repeated four times to increase the amount of loaded $Zn(OH)_2$ and were finally dried at room temperature. The modified samples were then treated with dry steam to facilitate the formation of ZnO phase. Fig. 1 represents a schematic representation for the modification process.

2.3. Determination of amount of MB in the synthetic wastewater and Zn content loaded C-100

Determination of MB was performed by measuring the absorbance water containing MB samples at λ_{max} = 665 nm using a UV/VIS spectrometer (Perkin—Elmer, Lambda 2). Total loaded Zn was carried out using a Perkin Elmer atomic absorption spectrophotometer with graphite furnace accessories (Model SIMAA 6000) and an electrodeless discharge lamp. The analysis carried out for the determination of loaded zinc ions indicates that the amount of loaded Zn^{2+} was found to be 0.4 g Zn/gm C-100 after four successive loading times.

2.4. Catalyst characterization

Slices of HCIX-Zn were characterized by scanning electron microscopy with energy-dispersive X-ray (scanning electron microscope (SEM)–energy-dispersive X-ray spectroscopy (EDX)) attachments (Model JEOL JSM-6360A).

The tunneling electron microscope (TEM) image was taken by a JEOL JEM-2200FS with a field emission gun under an accelerating voltage of 200 keV. The specimen was prepared by slicing Zn-HCIX with ultramicrotomy.

2.5. Adsorption studies

The adsorption kinetic studies were carried out by mixing a certain amount of Zn-HCIX with 200 ml

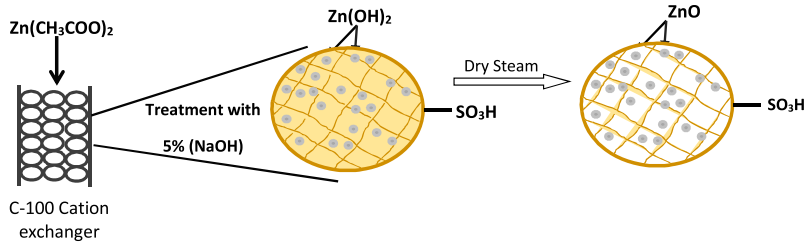

Fig. 1. Sketch of zinc loading process.

solution of methylene blue of 50, 75, 100, 150, and 300 mg L^{-1} concentrations followed by mechanical stirring using a shaker incubator at 150 RPM. In all cases, the working pH was that of solution and was not controlled. Mixtures were taken from the shaker at appropriate time intervals (5, 10, 15, 30, 45, 60, 90 min), and the left out concentration in the methylene blue solution was estimated. The amount of MB adsorbed at equilibrium per unit mass of resin, q_e, was calculated by:

$$q_e = \frac{(C_o - C_e) \times V}{m} \quad (1)$$

where V is the volume of MB solution in L; C_o and C_e are the initial and the equilibrium concentrations in mg/L, respectively; and m is the mass of adsorbent in grams.

2.6. Photocatalytic degradation test

Different doses of Zn-HCIX modified polymeric materials were suspended in synthesized MB dye solution, under permanent mechanical stirring and a constant flow of bubbled air, subjected to UV irradiation by immersing 6 W Hg lamp (254 nm) within the photoreactor (Fig. 2), where a total radiant flux (20 MW cm^2) was applied. The radiation flux was measured with a UV radiometer (Digital, UVX, 36). All measurements were performed at 25°C. At different time intervals, aliquot was withdrawn which was, subsequently, filtered through 0.45-μm (Millipore) syringe filter. Absorption spectra were recorded, and the rate of decolorization was observed in terms of change in intensity at 665 λ_{max} of the MB dyes. Similar experiments were carried out by varying the pH of the solution (pH 4–10), the initial concentration of MB dye (0.005 M), and the catalyst loading (0.05–0.2 g/l).

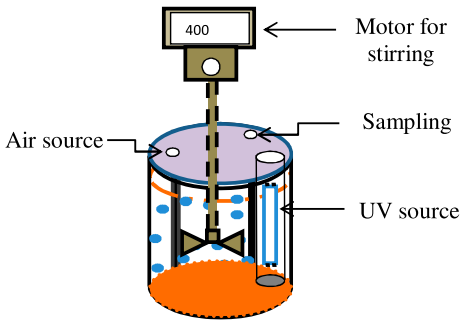

Fig. 2. Sketch of batch photoirradiation instrument.

3. Results and discussion

3.1. Catalyst characterization

3.1.1. X-ray diffraction (XRD)

Fig. 3 shows the typical X-ray diffraction (XRD) spectra for the synthesized ZnO which confirmed the wurtzite ZnO-type structures with different peak intensities, which further confirmed the formation of smaller particles. The relative intensity of the peaks of the obtained nanoparticles matches the bulk. The data obtained also show the effect of ZnO loading on the morphology of the synthesized ZnO nanoparticles with various loading ratios. In a typical synthetic process, the observed loaded ratios were changed by the number of loading process, although the final pH of the solution was the same.

3.1.2. Scanning electron microscope (SEM)

SEM images, as illustrated in Fig. 4(a) and (b), show practically no change in pore structure due to impregnation of Zn-HCIX. This observation reinforces that Zn-HCIX nanoparticles reside primarily in the gel phase and do not affect the resin pore structure. The interior fluid dynamics and tortuosity of the particles are unlikely to be affected after the dispersion of Zn-HCIX nanoparticles. The image also indicates the formation of nanorods; most of the nanorods have straight sides and regular ends, with average diameters range of 12–32 nm which were consistent with the

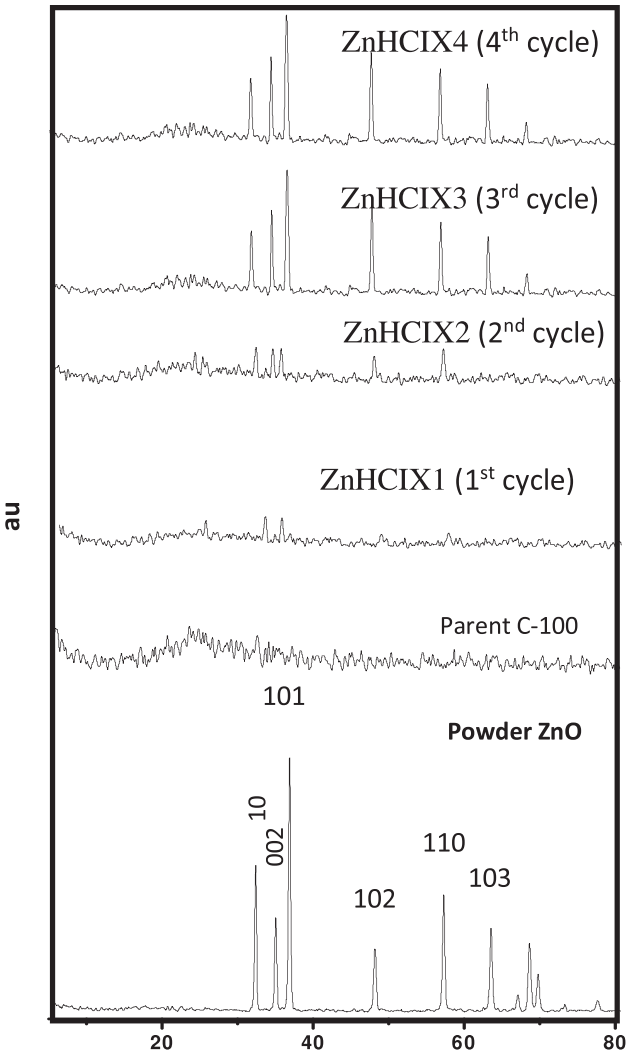

Fig. 3. XRD patterns of C-100 polymeric material modified with Zn cations in comparison with the powder ZnO.

crystallite size calculated by Scherrer's formula using the (100) and (002) diffraction peaks observed in XRD spectra.

Fig. 4(b) shows that the EDX mapping inside single hybrid particle-notice zinc is present throughout the entire bead. The data also indicate that ZnO is mainly located on the surface and decrease gradually upon going deep into the polymeric matrix as shown in Fig. 4(c).

3.1.3. Tunneling electron microscope (TEM)

The morphologies of Zn-HCIX crystallites and particles were also investigated by TEM as illustrated in Fig. 5. The light spots in the obtained image represent the polymeric matrix; however, the dark ones represent the loaded ZnO nanoparticles dispersed in the polymeric matrix with 22.5 average particle diameter.

3.2. Catalytic activity of Zn-HCIX

3.2.1. Adsorption of MB

As a part of degradation process, the adsorption behavior of MB using the synthesized Zn-HCIX was studied at different experimental conditions to determine the surface properties as well as the adsorption capacity of the catalyst.

3.2.1.1. Adsorption isotherm. Establishment of adsorption isotherm gives an essential aspect about the nature of adsorption process. Numerous isotherm equations have been reported, and three major isotherms, the Langmuir and Freundlich isotherms [22], are tested to fit the experimental data. The Langmuir isotherm has been successfully applied for a wide variety of adsorption processes which supposes adsorption occurred to homogeneous sites in the absorbent. It can be expressed as follows:

$$q_e = \frac{QK_L C_e}{1 + K_L C_e} \tag{2}$$

where Q is the adsorption capacity corresponding to form a complete monolayer and K_L is the Langmuir constant.

The basic parameters of Langmuir isotherm can be expressed by a dimensionless constant called separation factor or equilibrium parameter, R_L, defined by Weber and Chakkravorti [23] as:

$$R_L = \frac{1}{1 + K_L C_o} \tag{3}$$

The Freundlich isotherm, which is empirical for heterogeneous surface energy, is in the form:

$$q_e = K_F C_e^{\frac{1}{n}} \tag{4}$$

where K_F is the extent of the adsorption and n is the degree of nonlinearity between MB concentration n.

Fig. 6(a) and (b) represent the fitting of Langmuir adsorption isotherm at different temperatures and Zn loadings. The data obtained indicate the adsorption process is in a good fitting with Langmuir when

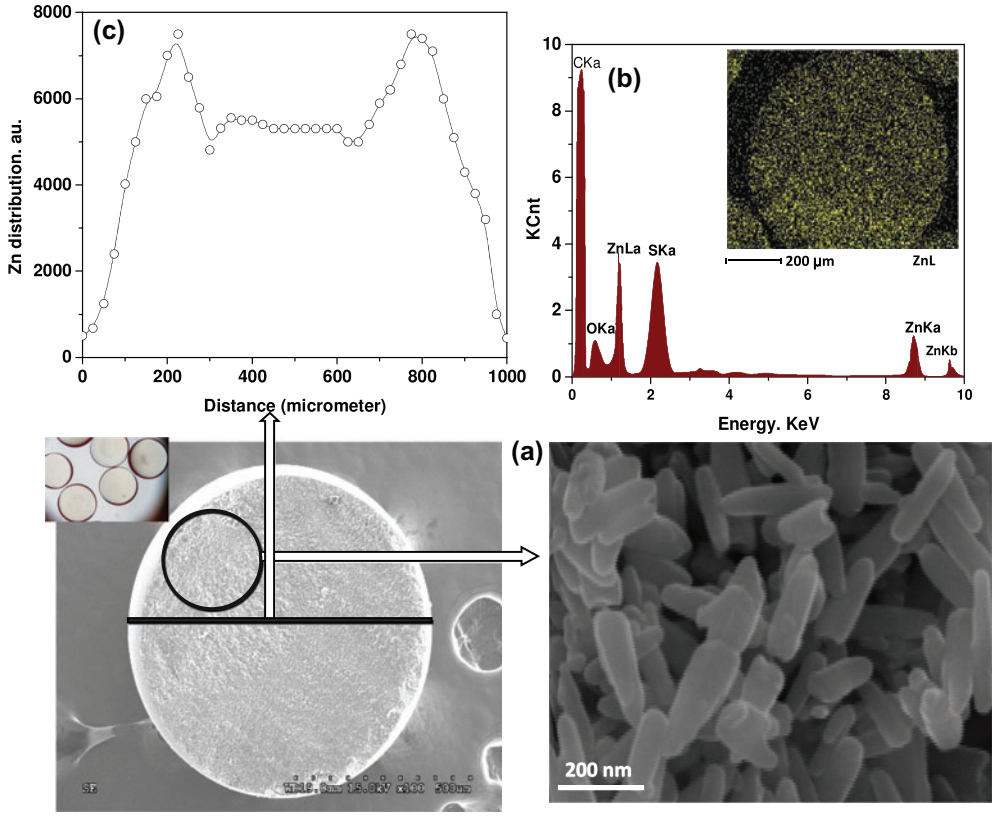

Fig. 4. (a) Purolite C-100 dispersed with ZnO nanoparticles (ZnHCIX), (b) Energy-dispersive X-ray (EDX) mapping of sliced Zn-HCIX particles (yellowish black dots represent zinc nanoparticles), and (c) Distribution of Zn nanoparticles on polymeric surface and pores.

compared with the Freundlich isotherm [24–26]. The related parameters have been summarized in Table 1. It is observed that the correlation coefficient (R^2) of Langmuir model is higher than the Freundlich, which means the adsorption belongs to the monolayer adsorption. All the R_L values were between 0 and 1, indicating that the adsorption of MB on the Zn-HCIX is favorable at the conditions being investigated. The data obtained in this study indicates that the adsorption process might involve chemisorption, through the replacement of Na^+ ions attached to the functional sulfonic acid groups of the resin (ion exchange) and the positively charged [$(CH_3)_2\,N^+$-] functional groups of methylene blue and physisorption through the hydrophobic–hydrophobic interaction of polymeric matrix and MB.

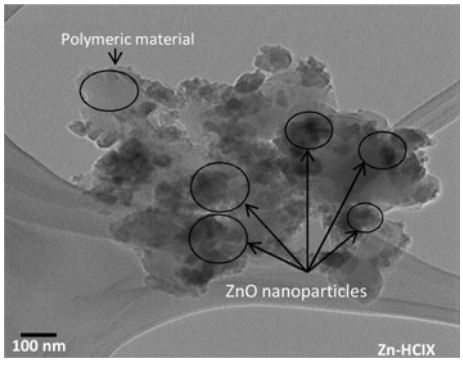

Fig. 5. TEM of sliced hybrid ZnO nanoparticles.

3.2.1.2. Adsorption thermodynamics. Table 2 includes the values of thermodynamic parameters such as free energy (ΔG°), enthalpy (ΔH°), and entropy (ΔS°) of adsorption which were calculated from the Langmuir constant "K" using the following relation:

$$\Delta G^\circ = -RT \ln K \tag{5}$$

$$\ln K = -\frac{\Delta H^\circ}{RT} + \text{Constant} \tag{6}$$

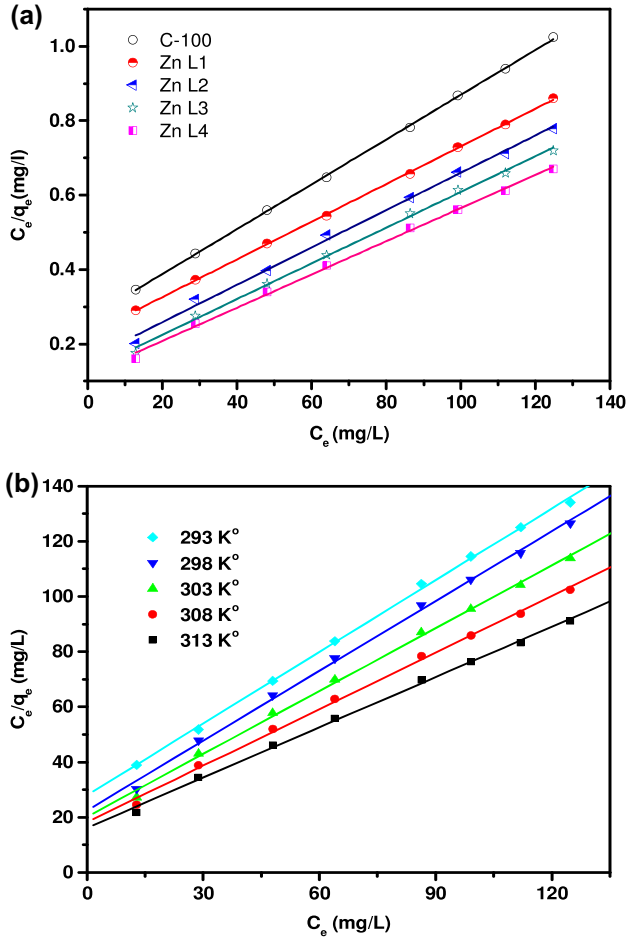

Fig. 6. Langmuir plots for MB adsorption onto HZnO at different (a) temperatures and (b) Zn loadings.

$$\Delta G^\circ = \Delta H^\circ - T\Delta S^\circ \quad (7)$$

The values of ΔH° and ΔS° were calculated from the slope and intercept of the linear variation of ln K with reciprocal of temperature ($1/T$) as depicted in Fig. 7. The values of ΔG° at different temperatures are positive which might predict the nonspontaneous behavior of methylene blue adsorption. The value of ΔH° calculated to be 26.9 KJ mol^{-1} indicates that the MB adsorption is governed by physisorption process. Furthermore, the calculated value of ΔS° was found to be 83 J K^{-1} mol^{-1}. The positive values of ΔS° (Table 2) show the increased disorder and randomness at the solid solution interface of methylene blue with Zn-HCIX adsorbent.

The values of ΔH° and ΔS° in methylene blue were found positive which indicates that the adsorption process has an endothermic behavior. All the results obtained for methylene blue adsorption using Zn-HCIX show best adsorption capacity upon increasing the amount of loaded Zn^{2+} at high temperatures.

3.2.2. MB photolysis

The effect of UV irradiation on the stability of MB toward degradation was investigated in the presence of different concentrations. The results indicate that MB exhibits different degradation rates depending on the concentration of MB used. The data also show that the lower the MB concentration is, the faster the degradation rate is, as depicted in Fig. 8(a).

3.2.3. Photocatalytic degradation

The catalytic activity of the synthesized Zn-HCIX catalyst was investigated by varying the different experimental conditions to get an idea about the reactivity of such kind of catalysts in the degradation of organic wastes in bench scale as well as industrial scale.

Fig. 8(b) illustrates the degradation of MB dye in the presence of Zn-HCIX/UV. The data obtained

Table 1
Calculated thermodynamic parameters for the effect of temperature on the adsorption of mb using ZN-HCIX

	Langmuir model				Freundlich model			
Temperature	q_{max} (mg/g)	K_L (L mg^{-1})	R_L	R^2	n	K_F [(mg/g) (mg/l)$^{1/n}$]	q_{max} (mg/g)	R^2
288	220	0.29	0.027	0.99	1.6	4.4	80	0.97
293	270	0.34	0.026	0.99	1.7	6.32	158	0.97
298	357	0.41	0.023	0.99	1.6	7.54	210	0.98
303	370	0.51	0.021	0.99	1.8	7.73	245	0.96
308	385	0.59	0.019	0.99	2.0	7.92	277	0.96

Table 2
Calculated thermodynamic parameters for the effect of temperature on the adsorption of MB using Zn-HCIX

	Thermodynamic parameters					
Temperature	K_L (L mg^{-1})	ln K	ΔG° (KJ mol^{-1})	ΔH° (KJ mol^{-1})	ΔS° (J K^{-1} mol^{-1})	R^2
288	0.29	−1.24	2.96	26.9	83	0.995
293	0.34	−1.1	2.63			
298	0.41	−0.9	2.21			
303	0.51	−0.67	1.69			
308	0.59	−0.53	1.35			

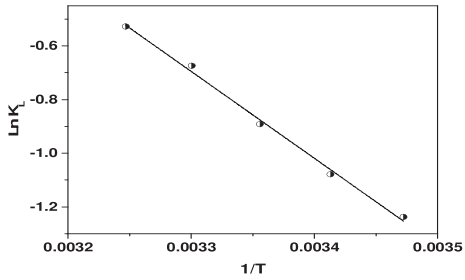

Fig. 7. Plot of ln K_L vs. $1/T$ for the adsorption process.

indicate that the used catalyst has a comparable efficiency as that obtained upon using of UV/H_2O_2 only. As indicated in Fig. 8(b), the complete removal of 0.05 mol/L MB consumes about 180 min in the presence of UV/H_2O_2; however, in case of Zn-HCIX/UV, consumed about 160 min.

The addition of H_2O_2 to Zn-HCIX/UV media exhibits excellent degradation rate since the complete removal of 0.05 mol/L MB was achieved within less than 5 min.

3.2.4. Effect of pH

The pH of the degradation medium is considered as one of the key factors that could affect the rate of degradation and possibly changes from one material to the other depending on the nature of the degraded materials. The investigations of pH changes effect on MB degradation indicate a disparate behavior, particularly in the first periods of the degradation process. The data illustrated in Fig. 8(c) indicate a marked increase in degradation rate upon varying the pH in the following order pH 4 > pH 8 < pH 10 < pH 6. The data also indicate that the rate of degradation at pH 10 during the initial periods is fast and diminishes gradually to reach steady state after 200 min from the start of irradiation process [20].

3.2.5. Effect of ZnO loadings

No doubt that the amount of loaded ZnO and doses play an important role in accelerating the degradation rate of MB but not for absolute limit. The data obtained for the effect of Zn-HCIX loading and dose were illustrated in Fig. 9(a) and (b). The figure shows that the increase in Zn-HCIX doses (0.1–0.4 gm/L) strongly affect the degradation rate with a complete MB mineralization time varying from 5 to 60 min according to the catalyst doses used. The increase in degradation rate with the increase in catalyst doses may be attributed to the increase in the formation upon the reaction of Zn-HCIX with the oxygen carrier materials which lead to further attack to the aromatic rings of MB causing the complete mineralization.

3.2.6. Effect of temperature

The effect of temperature on degradation rate was investigated within 15–35°C, and the obtained data were represented in Fig. 9(c). It is clear that the degradation rate is strongly affected by the raise of temperature to give a maximum degradation rate at 35°C reflecting the endothermic nature of the degradation process of MB. The data also indicate the complete disappearance of 0.01 M MB within less than 5 min.

The activation parameters associated with the decolonization of methylene blue are calculated from the plot of ln k_{obs} vs. $1/T$ (Fig. 10), which gives the value of activation E_a, according to the Arrhenius equation:

$$\ln K_{obs} = -\frac{\Delta E_a}{RT} + \ln A \quad (8)$$

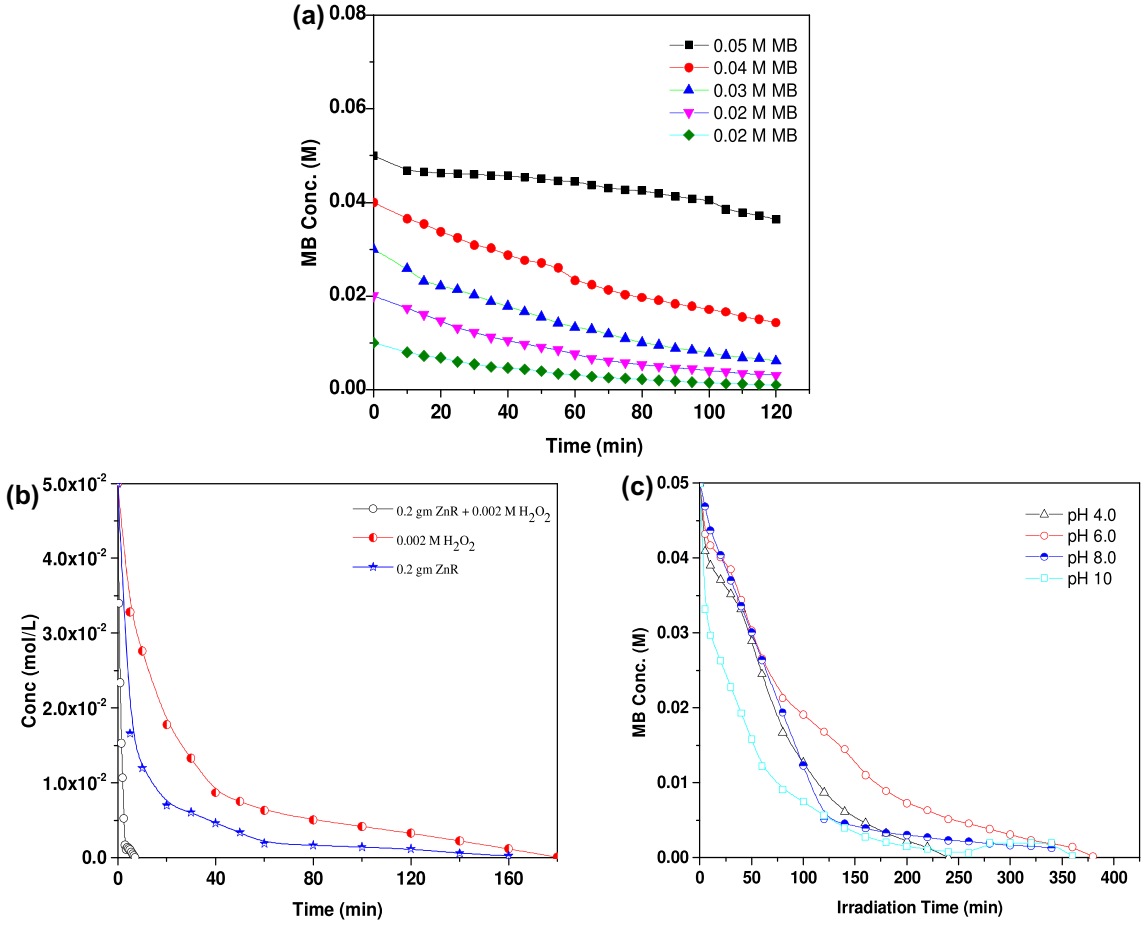

Fig. 8. Photodegradation of MB: (a) Different conc., (b) In presence of H_2O_2 and/or HZnO catalyst, and (c) At different pH.

The values of ΔH° and ΔS° can be calculated from the plot of the Eyring equation [25] as follows:

$$\ln \frac{K_{obs}}{T} = \ln \frac{k_B}{h} + \ln \frac{\Delta S^\circ}{R} - \frac{\Delta H^\circ}{RT} \quad (9)$$

where K_{obs} is the reaction rate constant, T is the absolute temperature, k_B is the Boltzman's constant (1.381×10^{-23} J K^{-1}), and h is the Plank's constant (6.626×10^{-34} J s). ΔS° is the entropy and ΔH° is the enthalpy.

From the linear plot of $\ln K_{obs}/T$ vs. T (Fig. 10), values of ΔH° and ΔS° can be calculated. The Gibbs' free energy ΔG° can, therefore, be calculated using Eq. (5). Thermodynamic parameters are given in Table 3. The positive values of ΔG° for the reaction (Table 3) indicate the nonspontaneous nature of decolorization of MB^+ by Zn-HCIX at the temperatures under investigation. The negative value of ΔS° suggest the decreased randomness at the liquid/solid interface during the decolorization of MB^+ solution by Zn-HCIX while the positive values of ΔH° show the endothermic nature of the reaction.

3.3. Kinetic study of the degradation process

The investigation of the degradation order of MB using Zn-HCIX catalyst was carried out under different experimental conditions, to understand the reaction passway, and the obtained data were illustrated in Fig. 11(a)–(c). It is clear that all reactions follow first-order kinetics and the calculated apparent rate constants indicate that the rate of degradation is directly proportional with the initial concentration of MB as well as Zn-HCIX doses.

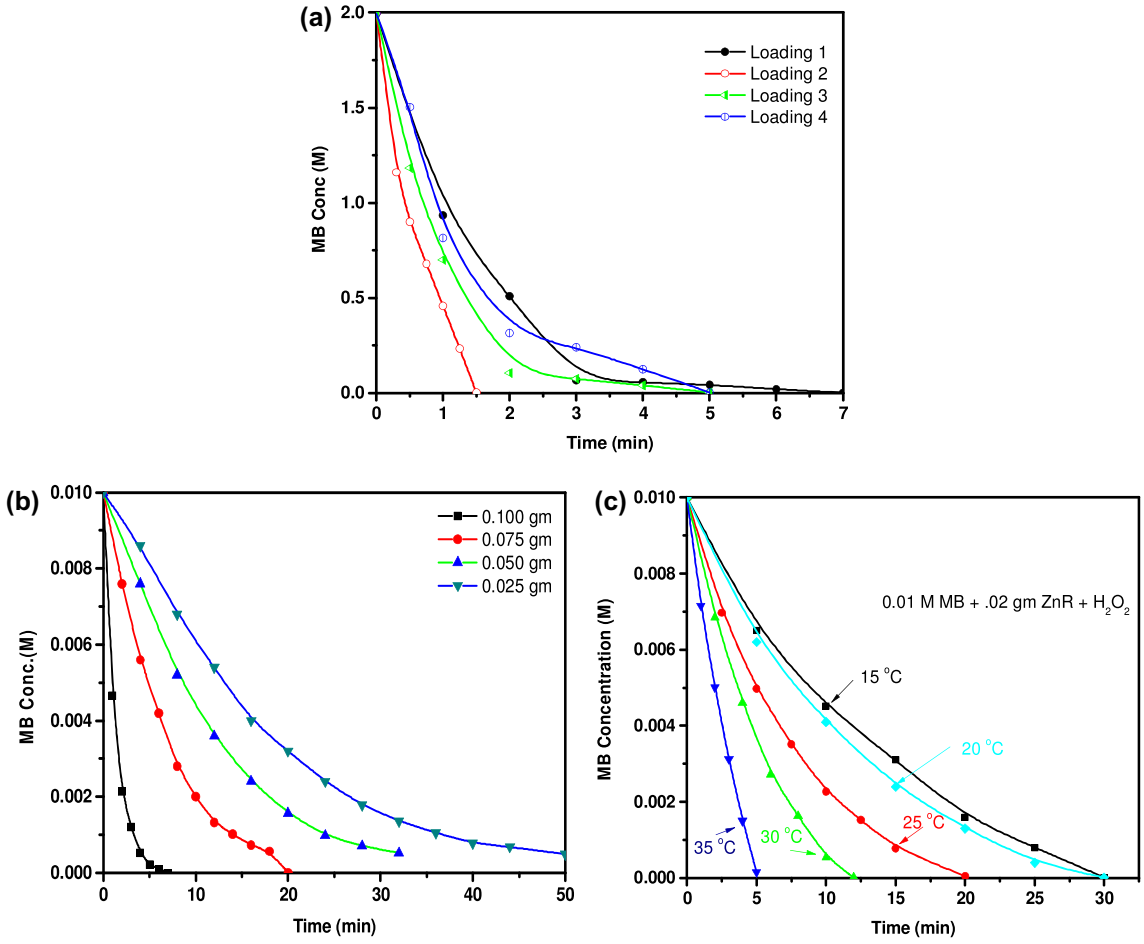

Fig. 9. Effect of different parameters on the photocatalytic degradation of MB: (a) Zn loading, (b) Zn doses, and (c) Temperatures.

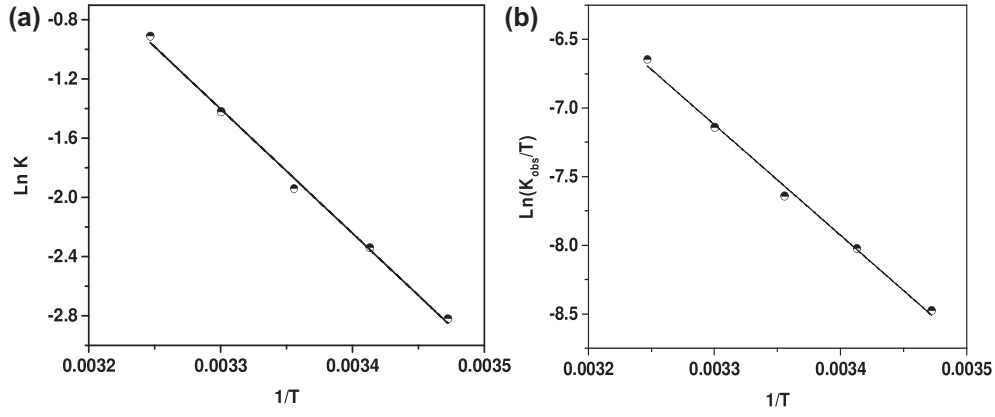

Fig. 10. (a) Plot of ln K vs. $1/T$ for the degradation process and (b) plot of ln (K_{obs}/T) vs. $1/T$ for degradation process.

Table 3
Calculated thermodynamic parameters for the effect of temperature on the degradation of MB using Zn-HCIX

	Thermodynamic parameters						
Temperature (K)	K_{obs} (min^{-1})	ln (K_{obs})	ln (K_{obs}/T)	ΔG° (KJ mol^{-1})	ΔH° (KJ mol^{-1})	ΔS° (J K^{-1} mol^{-1})	R^2
288	0.060	−2.82	−8.48	77.26	66.94	35.86	0.994
293	0.096	−2.34	−8.024	77.45			
298	0.143	−1.94	−7.642	77.63			
303	0.240	−1.42	−7.141	77.81			
308	0.400	−0.91	−6.65	77.98			

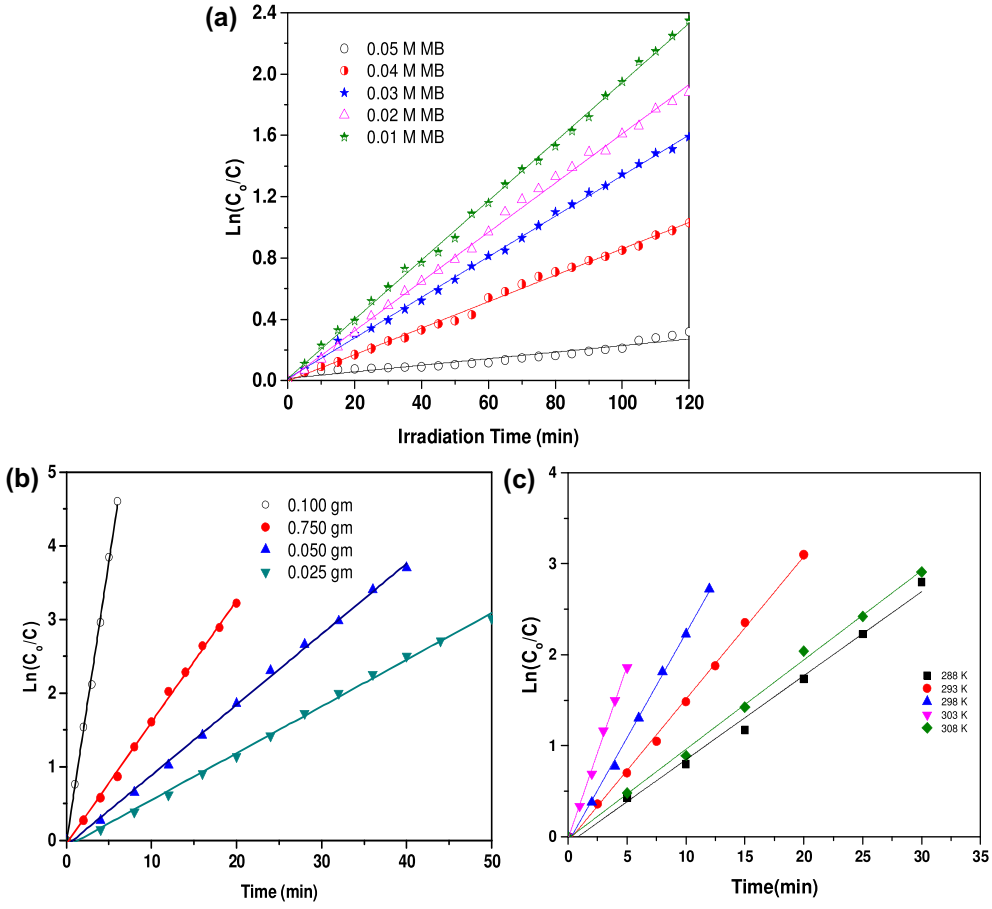

Fig. 11. ln (C_o/C) vs. time for the photodegradation of MB at different: (a) Conc. of MB, (b) Zn doses, and (c) Temperatures.

$$-\frac{d[MB]}{dt} = k[MB][Zn - HCIX] \quad (10)$$

Fig. 11(b) and (c) represent the ln (C_o/C) against time for the effect of catalyst doses and temperature on the degradation of MB. The data obtained reveal that the reaction rates follow first-order kinetics with different slopes depending on the temperature and the doses of catalyst used.

3.4. Large-scale water treatment

After determining the most suitable experimental conditions, 500 g of the synthesized Zn-HCIX catalyst have been applied added to water treatment tank as

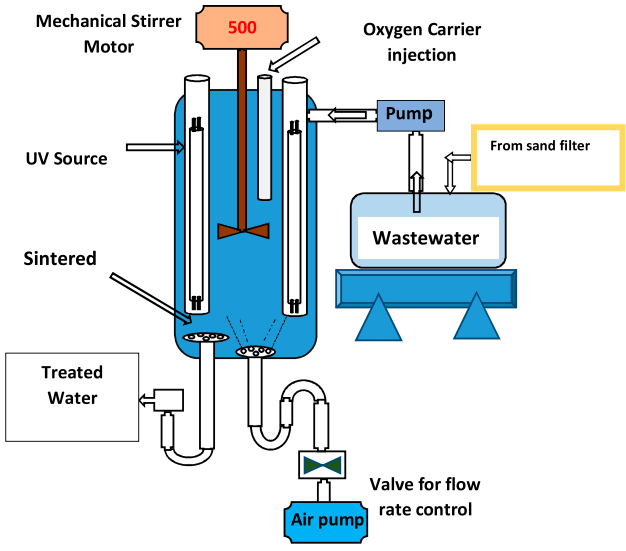

Fig. 12. Schematic illustration for large-scale water treatment.

described in Fig. 12 for large-scale pharmaceutical wastewater treatment. The data obtained indicate that the designed system can treat more than 20 m^3/d with a complete methylene blue removal.

4. Conclusion

The modification of C-100 cation exchanger with Zn cation was performed to enhance the photocatalytic activity of the synthesized materials via spreading ZnO on large surface area polymeric materials. The synthesized materials were treated with roasted water vapor to facilitate the formation of ZnO phase. The catalytic activity of the synthesized materials was studied in the photodegradation of MB dye, and the obtained data indicate that the used materials exhibit a very good removal behavior of methylene blue dye under the regular experimental conditions. Furthermore, the most efficient experimental conditions were examined on real wastewater samples containing methylene blue dye as well as some other dyes, and the obtained data indicate the efficiency of the synthesized materials to treat more than 20 m^3/d polluted water.

Abbreviations

ZnO	—	zinc oxide
MB	—	methylene blue
HCIX	—	hybrid cation exchanger
Zn-HCIX	—	zinc loaded hybrid cation exchanger
Zn-HCIX1	—	indicates the number of Zn loading
XRD	—	X-ray diffraction
SEM	—	scanning electronic microscope
EDX	—	energy-dispersive X-ray
TEM	—	the tunneling electron microscope

References

[1] K. Rajeshwar, M.E. Osugi, W. Chanmanee, C.R. Chenthamarakshan, M.V.B. Zanoni, P. Kajitvichyanukul, R. Krishnan-Ayer, Heterogeneous photocatalytic treatment of organic dyes in air and aqueous media, J. Photochem. Photobiol. C 9 (2008) 171–192.
[2] M.A. Rauf, S.S. Ashraf, Fundamental principles and application of heterogeneous photocatalytic degradation of dyes in solution, Chem. Eng. J. 151 (2009) 10–18.
[3] F. Han, V.S.R. Kambala, M. Srinivasan, D. Rajarathnam, R. Naidu, Tailored titanium dioxide photocatalysts for the degradation of organic dyes in wastewater treatment: A review, Appl. Catal. A 359 (2009) 25–40.
[4] H. Yoneyama, T. Torimoto, Titanium dioxide/adsorbent hybrid photocatalysts for photodestruction of organic substances of dilute concentrations, Catal. Today 58 (2000) 133–140.
[5] Y.Z. Li, W. Xie, X.L. Hu, G.F. Shen, X. Zhou, Y. Xiang, X.J. Zhao, P.F. Fang, Comparison of dye photodegradation and its coupling with light-to-electricity conversion over TiO_2 and ZnO, Langmuir 26 (2010) 591–597.
[6] Y.X. Chen, S.Y. Yang, K. Wang, L.P. Lou, Role of primary active species and TiO_2 surface characteristic in UV-illuminated photodegradation of acid Orange 7, J. Photochem. Photobiol A 172 (2005) 47–54.
[7] N. Dizge, C. Aydiner, E. Demirbas, M. Kobya, S. Kara, Adsorption of reactive dyes from aqueous solutions by fly ash: Kinetic and equilibrium studies, J. Hazard. Mater. 150 (2008) 737–746.
[8] D.M. Chen, Z.H. Wang, T.Z. Ren, H. Ding, W.Q. Yao, R.L. Zong, Y.F. Zhu, Influence of defects on the photocatalytic activity of ZnO, J. Phys. Chem. C 118 (2014) 15300–15307.
[9] C. Xu, G.P. Rangaiah, X.S. Zhao, Photocatalytic degradation of methylene blue by titanium dioxide: Experimental and modeling study, Ind. Eng. Chem. Res. 53 (2014) 14641–14649.
[10] S.J. Xia, L.Y. Zhang, G.X. Pan, P.P. Qian, Z.M. Ni, Photocatalytic degradation of methylene blue with a nanocomposite system: Synthesis, photocatalysis and degradation pathways, Phys. Chem. Chem. Phys. 17 (2015) 5345–5351.
[11] H.L. Wang, D.Y. Zhao, W.F. Jiang, VIS-light-induced photocatalytic degradation of methylene blue (MB) dye using PoPD/TiO_2 composite photocatalysts, Desalin. Water Treat. 51 (2013) 2826–2835.
[12] R.H. Chen, H.T. Qiao, Y. Liu, Y.H. Dong, P. Wang, Z.H. Zhang, T. Jin, Adsorption of methylene blue from an aqueous solution using a cucurbituril polymer, Environ. Prog. Sustainable Energy 34 (2015) 512–519.
[13] S. Chatterjee, A. Kumar, S. Basu, S. Dutta, Application of response surface methodology for methylene blue dye removal from aqueous solution using low cost adsorbent, Chem. Eng. J. 181–182 (2012) 289–299.

[14] A. Simi, V. Azeeza, Removal of methylene blue dye using low cost adsorbent, Asian J. Chem. 22 (2010) 4371–4376.
[15] K. Elass, A. Laachach, A. Alaoui, M. Azzi, Removal of methylene blue from aqueous solution using ghassoul, a low-cost adsorbent, Appl. Ecol. Environ. Res. 8 (2010) 153–163.
[16] M. Shanthi, V. Kuzhalosai, Photocatalytic degradation of an azo dye, acid red 27, in aqueous solution using nano ZnO, Indian J. Chem. A 51 (2012) 428–434.
[17] A. Khanna, K.V. Shetty, Solar light-driven photocatalytic degradation of anthraquinone dye-contaminated water by engineered Ag@TiO_2 core-shell nanoparticles, Desalin. Water Treat. 54 (2015) 744–757.
[18] X.H. Liu, Y.L. Yang, X.X. Shi, K.X. Li, Fast photocatalytic degradation of methylene blue dye using a low-power diode laser, J. Hazard. Mater. 283 (2015) 267–275.
[19] A. Umar, M.S. Akhtar, A. Al-Hajry, M.S. Al-Assiri, G.N. Dar, M.S. Islam, Enhanced photocatalytic degradation of harmful dye and phenyl hydrazine chemical sensing using ZnO nanourchins, Chem. Eng. J. 262 (2015) 588–596.
[20] M.M. El-Moselhy, N.M.R. Mahmoud, M.M. Emara, Copper modified exchanger for the photodegradation of methyl orange dye, Desali. Water Treat. 52 (2014) 7225–7234.
[21] Y. Bulut, H. Karaer, Adsorption of methylene blue from aqueous solution by crosslinked chitosan/bentonite composite, J. Dispersion Sci. Technol. 36 (2015) 61–67.
[22] B. Kiran, A. Kaushik, Chromium binding capacity of Lyngbya putealis exopolysaccharides, Biochem. Eng. J. 38(1) (2008) 47–54.
[23] T.W. Weber, R.K. Chakkravorti, Pore and solid diffusion models for fixedbed adsorbers, AIChE J. 20 (1974) 228–238.
[24] M. Peydayesh, A. Rahbar-Kelishami, Adsorption of methylene blue onto platanus orientalis leaf powder: Kinetic, equilibrium and thermodynamic studies, J. Ind. Eng. Chem. 21 (2015) 1014–1019.
[25] P.P. Remy, M. Etique, A.A. Hazotte, A.S. Sergent, N. Estrade, C. Cloquet, K. Hanna, F.P.A. Brand, Pseudo-first-order reaction of chemically and biologically formed green rusts with Hg-II and $C_{15}H_{15}N_3O_2$: Effects of pH and stabilizing agents (phosphate, silicate, polyacrylic acid, and bacterial cells), Water Res. 70 (2015) 266–278.
[26] Y.S. Ho, Comments on "Adsorption of 2-mercaptobenzothiazole from aqueous solution by organo-bentonite" by P. Jing, MH Hou, P. Zhao, XY Tang, HF Wan. J. Environ. Sci. 26(12) (2014) 2571–2572.